Quantitative measuring methods applied for the mixing phenomena of film cooling

K. Takeishi, M. Komiyama & Y. Oda
Department of Mechanical Engineering, Osaka University, Japan

Abstract

In this paper, the quantitative measuring methods of Pressure Sensitive Paint (PSP), acetone Laser Induced Fluorescence (LIF) and Particle Image Velocimetry (PIV) are presented for the measuring of a complicated mixing flow field of film coolant and a mainstream. The time-averaged film cooling effectiveness was accurately measured with the PSP method, when precise calibration has been conducted. Instantaneous distributions of velocity vectors and film cooling effectiveness were measured simultaneously near the exit of circular hole by acetone LIF and PIV. The simultaneous measurement is very useful not only to clear the spatial flow field of film cooling but also to confirm the accuracy of numerical simulations of film cooling.
Keywords: film cooling, gas turbine, PSP, acetone LIF, PIV.

1 Introduction

Gas turbines are used for aircraft propulsion and land-based power generation. Developments in turbine cooling technology play a crucial role in increasing the thermal efficiency and power output of advanced gas turbines. Gas turbine's blades and vanes are cooled externally by film cooling in high temperature gas turbines. It is achieved by injecting relatively cooler air from the internal coolant passages out of the blade surface in order to form a protective layer between the blade surface and hot gas-path flow. The interaction between film-cooling air and mainstream, which is representative of film cooling, forms a shear layer that leads to mixing and a decay of the film cooling performance along a blade surface.

It is well known that jet vortices are generated due to the friction of a film cooling air jet flow and a main stream cross-flow. A large number of papers have

WIT Transactions on Engineering Sciences, Vol 83, © 2014 WIT Press
www.witpress.com, ISSN 1743-3533 (on-line)
doi:10.2495/HT140421

been published with the visualization or numerical works of these vortices. Fric and Roshko [1] studied experimentally vortical structures in the wake of the transverse jet at high blowing ratios. They classified the vortical structures into a shear layer, horseshoe and wake vortices and a counter rotating vortex pair. Jovanovic *et al*. [2] illustrated Figure 1 which shows vortical structures generated by means of jet cross-flow interaction with film cooling characteristics. Morton and Ibbetson [3] analyzed the warp mechanism of the vortical structures. The literature written on film cooling mainly focuses on film cooling effectiveness and heat transfer coefficient, mostly time averaged with few exceptions. There are few quantitative experimental studies that focus attention on the detailed flow structure which control film cooling effectiveness resulting from the jet-mainstream interaction near film cooling holes. Recently, Kumagai *et al*. [4] measured the mixing flow field of a film cooling flow by LIF (Laser Induced Fluorescence) and Coletti *et al.* [5] measured the exiting jet flow through film cooling holes on blade pressure surface of trailing edge by using MRI (Magnetic Resonance Imaging) method. Sakai *et al*. [6] conducted precise analysis of the mixing flow field of an inclined film cooling flow and a main stream cross-flow by LES (large Eddy Simulation).

In this paper, the film cooling effectiveness was measured by PSP (Pressure Sensitive Paint) and the characteristics of instantaneous mixing field of film cooling air with mainstream were investigated by acetone LIF and PIV (Particle Image Velocimetry) quantitatively. The usefulness of such quantitative measuring methods not only for the investigation of film cooling phenomena but also for the confirmation of the accuracy of the numerical simulations will be presented.

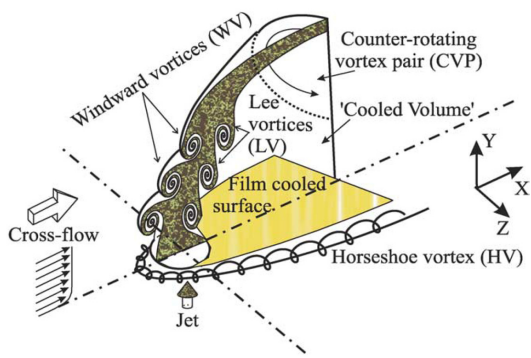

Figure 1: Interaction of film cooling jet through a circular hole with mainstream.

2 Experimental test facility

The present experiment has been conducted using a scale-up model of film cooling holes installed on the bottom surface of a low-speed wind tunnel in order to allow detailed probing of flow features. The wind tunnel is an open-circuit and

subsonic flow can be produced through an inlet nozzle with a 9:1 contraction ratio [4]. At the inlet of the nozzle section, there were honeycomb and screen. Therefore, the airflow has low turbulence intensity and uniform velocity profile at the entrance of the test section. The test section is 300 mm wide, 300 mm height, and 1950 mm long. The air speed inside the test section can be varied from 0 to 40 m/s. For the free-stream velocity of 20 m/s, the flow at the test section shows excellent spatial uniformity, with free stream turbulence intensity less than 0.36%. A film cooling hole is located 950 mm downstream from the exit of the contraction section.

The geometry of film cooling hole is circular and the guide channels to the exits of film cooling hole were inclined at 30 degree toward the main flow direction. It was made of low thermal conductivity material (Sanyo-chemical SanmodurMS) to reinforce adiabatic condition. The diameter of the guide channel, d, was 5 mm.

3 PSP method

In this study, PSP was used for measuring the film cooling effectiveness distribution on the wall. PSP is an optical pressure sensor. It uses a special pigment that changes its luminescence intensity upon reaction with oxygen molecules. The change of luminescence intensity is attributed to the optical quenching of the pigment due to oxygen molecules. Before starting the film cooling tests, calibration tests were conducted using a PSP-painted plate whose temperature was controlled by Joule heating in a closed chamber. The luminescence intensity from the PSP was measured for various combinations of oxygen concentrations in the chamber and temperatures of the PSP-painted plate, and calibration curve, shown in Figure 2, was obtained to estimate the oxygen concentration from the measured luminescence intensity and temperature.

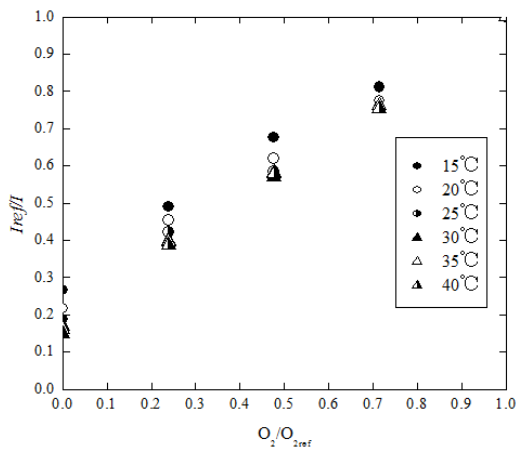

Figure 2: Calibration curve of PSP Emission Intensity on temperature and Oxygen concentration.

Three images were captured: 1) a background image with no main stream and no film cooling flow in darkness, 2) an image with the main stream but no film cooling flow, and 3) an image with both the main stream and the film cooling flow. The first image was used to calibrate each pixel of the CCD camera's sensor, whereas the second and third images were used to correct the unevenness of the light emitted from the LEDs. Twenty images were captured in each case, and they were averaged. The PSP's luminescence intensity is affected by its temperature, and, hence, the temperature of the wall during experimentation was monitored using K-type thermocouples.

By using air (21% oxygen concentration) for the main stream and nitrogen (0% oxygen concentration) for the film cooling jet, the concentration distribution of oxygen, which is determined by the mixing of the main stream (air) and coolant (nitrogen), can be measured on the wall downstream of the film cooling hole. The film cooling effectiveness was defined by the following equation:

$$\eta = \frac{T_\infty - T_{aw}}{T_\infty - T_c} \tag{1}$$

where T_∞ and T_c are the temperatures of the main stream and coolant in the plenum, respectively, and T_{aw} is the adiabatic wall temperature.

Then, using an analogy between heat and mass transfer, Eq. (1) is modified to Eq. (2).

$$\eta = \frac{C_\infty - C_w}{C_\infty - C_c} \tag{2}$$

where C_∞ and C_c are concentration of the oxygen in the main stream and plenum chamber, respectively; C_w is the concentration of the oxygen in the film-cooling air just above the wall.

The blowing ratio, which is defined as Eq. (3), was controlled by changing the film-cooling air flow rate.

$$M = \frac{\rho_c u_c}{\rho_\infty u_\infty} \tag{3}$$

Figure 3 shows an optical measurement system to measure film cooling effectiveness with PSP. The wall of the wind tunnel is painted with PSP (ISSI PtTfPP FIB-UF405). Pure nitrogen gas for film cooling is supplied from a nitrogen gas tank and the density ratio is DR = ρ_c/ρ_∞ = 0.967 through the whole PSP experiments. Thus, C_c and C_∞ are 0% and 21%, respectively, and C_w is measured using the following method. LED light sources with a wavelength of 405 nm were used as an excitation light source. Images were captured using a CCD camera (Hamamatsu Photonics, C9440-05C, 1344 × 1024 pixels, 12-bit) located at opposite the PSP-painted wall, as shown in Figure 3. Here, light, except phosphorescence with the wavelength of 650 nm, was cut off by a band

pass filter. The images were digitally stored on hard disks using HIPIC 8.30, an image acquisition software application. Figure 4 shows the comparison of film cooling effectiveness measured by PSP method and thermocouples respectively. It is confirmed from Figure 4 that they fit very well and heat and mass transfer analogy is held.

Using the partial derivative method described by Moffat [7], an uncertainty analysis was performed on the film cooling effectiveness measured by PSP. The PSP method is temperature-sensitive. In this experiment, the maximum error of temperature measurement was within ±0.1°C, and it affected the uncertainty of film cooling effectiveness by ±0.7%. Consequently, the total experimental uncertainty adds up to 1.6% in the area where the film cooling effectiveness, but it is 7.2% in the area corresponding to $\eta = 0.1$ because the phosphorescence light becomes weak in areas having film cooling effectiveness less than 0.1.

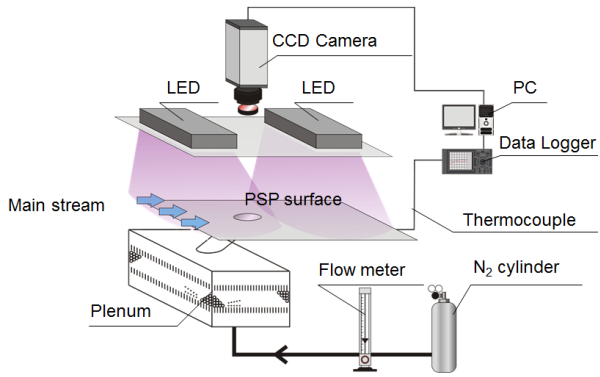

Figure 3: Optical measurement system to measure film cooling effectiveness with PSP.

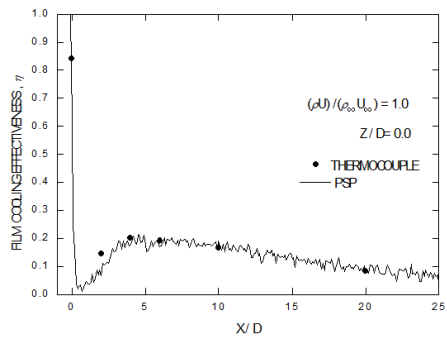

Figure 4: Comparison of film cooling effectiveness measured by PSP and thermocouple.

4 Acetone LIF method

LIF is a method for measuring concentrations in gaseous flows. The advantages of LIF are non-intrusiveness, instantaneousness, and high fluorescence intensity. In addition, LIF can realize high spatial resolution for the tracer concentration field. The flow is illuminated by a laser sheet of a wavelength that is tuned to excite a specific absorption transition of a molecular tracer, which is added for this purpose. A few of the molecules in the lower energy level absorb the incident light and are excited to a higher energy state. When the excited state returns to the lower-energy state, fluorescence light is emitted with a different wavelength from that of the incident light. Thus, fluorescence light from the tracer can be extracted easily from the scattered light using an interference filter.

If the thermal diffusivity of air and the mass diffusivity of the tracer are close, thermal diffusion can be replaced by mass transfer based on the heat/mass transfer analogy. Thus, the local non-dimensional temperature can be calculated using equation (4).

$$\theta = \frac{T_\infty - T}{T_\infty - T_c} = \frac{C_\infty - C}{C_\infty - C_c} \tag{4}$$

Lozano *et al.* [8] showed that acetone is one of the tracers used for concentration measurements in gaseous flows with LIF, and the ratio between acetone vapor's mass diffusion coefficient through air, D, and the thermal diffusivity of standard air, α, is about 2.0 (D = 11.2 mm^2/s, α = 22.3 mm^2/s) [9]. This is close enough for applying the heat/mass transfer analogy. In addition, acetone's LIF is known to show good linearity with respect to the partial pressure of acetone in atmospheric pressure gas. Table 1 shows the optical property of acetone and Figure 5 shows the thermal property of acetone, such as vapor pressure of acetone versus temperature and absorption cross-section of acetone versus illuminated wave length. It is known 275 nm wavelength is best, however in our study an Nd:YAG laser of 266 nm wavelength was used as the excitation light source. Figure 6 shows the calibration test results which shows good linearity of acetone LIF intensity versus acetone mole fraction. Thus, we use acetone as the tracer to measure the spatial non-dimensional concentration distribution with the LIF method.

The beam was expanded to a sheet of having a width of 25 mm and a thickness of 1 mm using four cylindrical lenses passing through the test section, as shown schematically in Figure 7 [4]. Saturated acetone vapor in air is produced by bubbling air in bottles containing acetone liquid. For obtaining the optimal acetone vapor concentration, dry air is mixed with acetone-vapor-saturated air in a scheduled ratio [10].

An uncertainty analysis was performed on the measurements of the non-dimensional concentration, θ, based on the uncertainties associated with the measured calibration curve of the LIF intensity, acetone-mixing air temperature, and film-cooling air flow rate, and the total uncertainty in the local non-dimensional concentration was found to be $\delta\theta = \pm 6.2\%$.

Table 1: Photophysical property of acetone.

	B.P.	Absorption	σ_{max}($\times 10^{-20}$cm^2)	φ	Emission	τ
Fluorescence	56℃	225-320nm	4.7	0.20%	350-550nm	4ns
Phosphorescence				1.80%	350-600nm	200μs

Absorption : Absorption spectrum
B.P. : Boiling point
Emission : Emission spectrum
σ_{max} : Maximum absorption cross section
τ : Lifetime
φ : Quantum efficiency

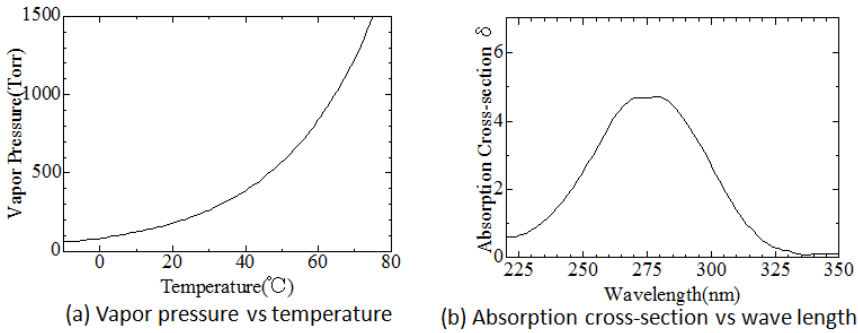

Figure 5: Thermal property of acetone.

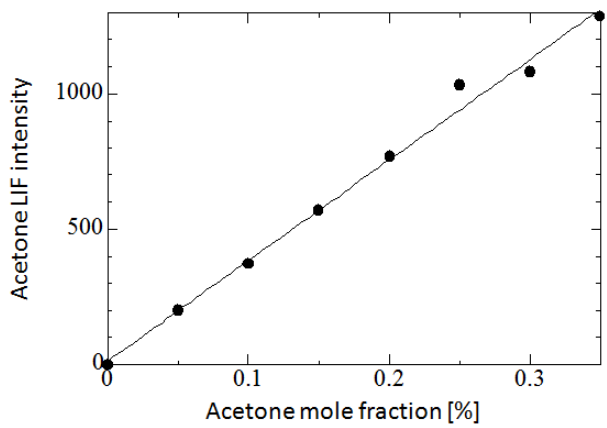

Figure 6: LIF intensity of acetone with parameter of mole fraction.

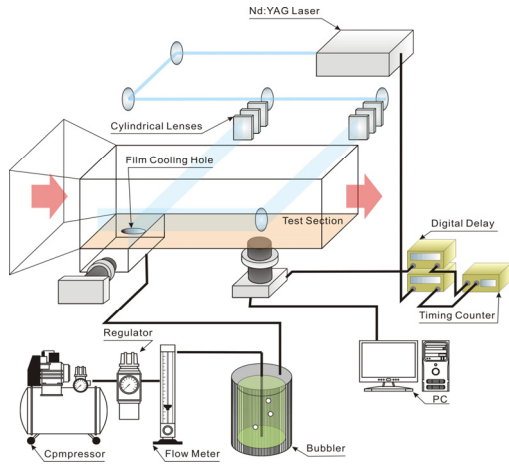

Figure 7: Optical measurement system of acetone LIF to measure spatial concentration distribution of acetone.

5 PIV method

PIV was used to capture instantaneous velocity fields. The secondary flow blowing through film cooling holes contains fine particles of olive oil as a tracer, which are about 1μm in diameter. The particles of olive oil were generated by bubbling compressed air into a pool of olive oil through a Raskin nozzle in a pressure vessel. In the vessel, air bubbles burst at the olive-oil/air interface, and about 1μm olive oil particles are released into the air. A dual-pulsed Nd:YAG laser, of wavelength 532 nm, was employed to illuminate the tracers. Three cylindrical lenses were used to form a laser sheet. The laser sheet was guided by a mirror located downstream to illuminate the test window. The particle pattern formed by the light reflected on the particle surfaces were taken with a CCD camera located at the side of the test section and the images were digitally stored on hard disks using the acquisition software HIPIC 8.0. To reduce the effect of reflection from the bottom surface, a background image for each pulse is subtracted from each frame to eliminate the effect of laser light reflection. The pairs of captured images were processed by a recursive local-correlation method to obtain velocity vector fields.

6 Results and discussion

Figure 8 shows the adiabatic film cooling effectiveness contours of a circular hole at $M = 0.5$, 1.0 and 1.5 measured by PSP method. In the case of the blowing ratio of $M = 0.5$, the surface is covered with film cooling air because the penetration of the film jet into the mainstream is weak and the film jet is bent to the wall direction by the mainstream. In the case of flow at $M = 1.0$ shown in Figure 8, the film cooling effectiveness just downstream the film cooling hole

shows very low value. The reason of this low value is the lift off effect of film cooling jet into the main stream. At the downstream, the film cooling air is bent to the wall direction by the mainstream and reattaches on the surface near $x/d = 3$ and the film cooling effectiveness recovers to about 0.2. In case of increasing the blowing ratio M to 1.5, the film cooling jet penetrates into the mainstream and the film cooling effectiveness on the wall is almost zero.

As it is clear from Figures 4 and 8, PSP method is an accurate quantitative method to measure the film cooling effectiveness when precise calibration has been conducted.

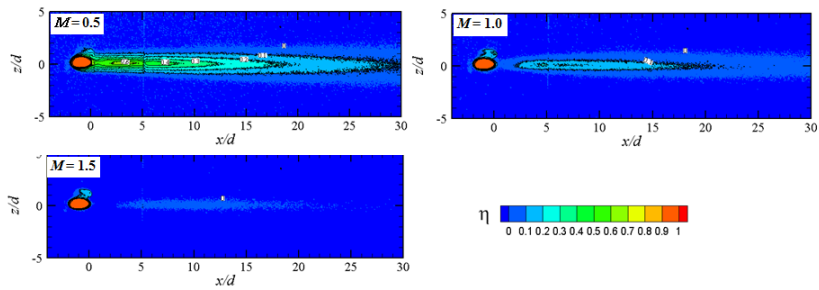

Figure 8: Film cooling effectiveness measured by PSP.

Figures 9 and 10 show the time-averaged film cooling effectiveness distribution at $z/d = 0$ and the cross sections at selected locations obtained by acetone LIF near the exit of a circular hole, for blowing ratio of $M = 1.0$. Figure 10 is a view from upstream. It appeared from Figure 9 that at low blowing ratio of $M = 0.5$, the film cooling air jet adheres on the wall and attains high film cooling effectiveness as it is clear from Figure 8. However, the penetration of the film cooling jet into mainstream was enhanced by increasing the coolant blowing ratio M and therefore the film cooling effectiveness decreased. Figure 10 clearly shows the generation of kidney vortex structure at $x/d = 2$, and there occurs an entrainment of mainstream hot gas into the gap between the film cooling jet and the wall.

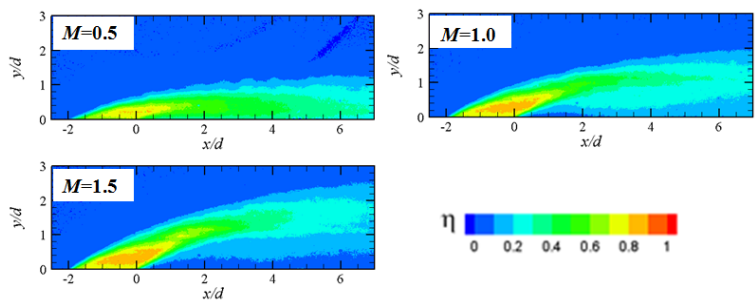

Figure 9: Film cooling effectiveness measured by acetone LIF at $z/d = 0$ section.

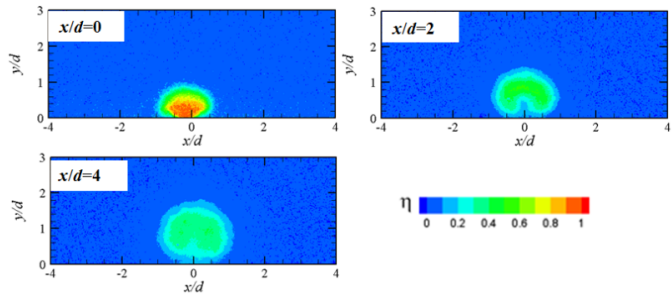

Figure 10: Cross section film cooling effectiveness measured by acetone LIF at $M = 1.0$.

Figures 11 and 12 show the time-averaged velocity vectors and vorticity distribution measured at $M = 1.0$ by PIV method. As it is clear from Figure 11, a quite low velocity region and a shear layer was detected downstream the circular film cooling hole exit, and penetration of the film cooling jet into mainstream was clearly detected. Figures 12 shows the time-averaged velocity vectors and vorticity distribution measured for circular film cooling hole at $M = 1.0$ by PIV method. The generation of kidney vortex structure is clearly captured.

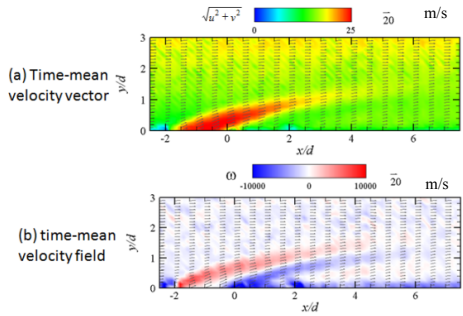

Figure 11: Time-mean velocity vector and time-mean velocity field at $z/d = 0$ and $M = 1.0$.

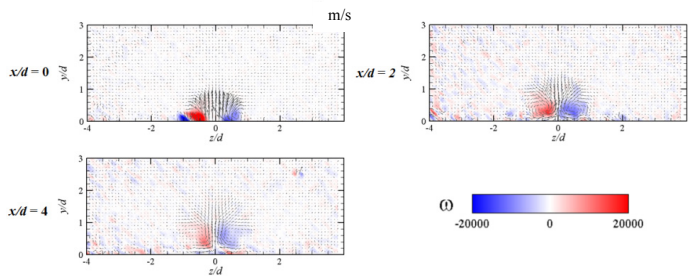

Figure 12: Time-mean velocity field of film cooling mixing field at $M = 1.0$.

Figure 13 shows instantaneous and simultaneous distributions of velocity vectors and film cooling effectiveness near the exit of circular hole measured by acetone LIF and PIV at M = 0.5 and 1.0. The arrows represent the velocity vectors in the z/d = 0 planes. And the colour contour shows the film cooling effectiveness. Positive vertical components of velocity were observed at the exit of cooling hole at $-2 < x/d < -1$ at M = 1.0. This indicates that the cooling air jet penetrates into the mainstream. Further downstream but still over the exit of the circular hole, the velocity vectors show a stronger penetration and the measured vertical velocities were positive at the downstream of the cooling hole (between $2 < x/d < 4$). This indicates that some of the mainstream fluid is ingested under the film cooling air and elevated the film cooling air. The film cooling air through circular film cooling hole is lifted from the surface.

As shown in Figure 13, a shear layer with large velocity gradients can be seen behind the downstream. This shear layer makes a complex boundary between the film core and mainstream. The shape and velocity gradients of this shear layer are influenced by the blowing ratio. The Kelvin-Helmholtz instability was generated and grown up along the turbulent shear layer. The detail mixing phenomena generated by Kelvin-Helmholtz instability in the turbulent shear layer was successfully captured by the present simultaneous measurement of velocity and concentration fields with PIV and acetone LIF.

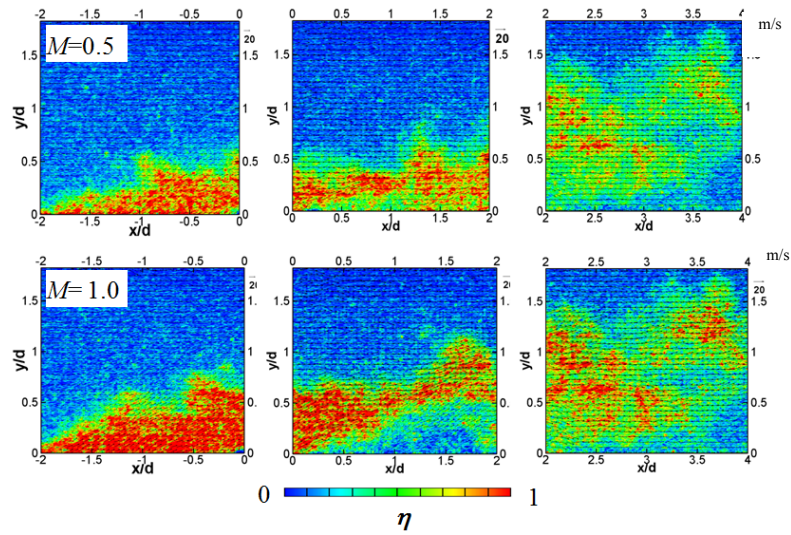

Figure 13: Instantaneous and simultaneous distributions of velocity vectors and film cooling effectiveness measured by acetone LIF and PIV at z/d = 0 and M = 1.0.

The averaged spatial distribution of film cooling effectiveness and velocity vectors measured by acetone LIF and PIV as show in Figures 9, 10, 11 and 12, and the instantaneous and simultaneous distributions of velocity vectors and film

cooling effectiveness near the exit of circular hole measured by acetone LIF and PIV as shown in Figure 13 are very valuable and useful data not only to understand the mixing phenomena between the film cooling air jet and the mainstream but also to confirm the accuracy of numerical analysis adopted to solve such a very complicated flow field.

7 Conclusions

In this paper, the mixing flow fields of a film cooling air with a mainstream have been investigated by using PSP, acetone LIF, and PIV for an inclined circular hole. As a result, by using acetone LIF and PIV measurement, detailed time-mean and instantaneous spatial profile of film effectiveness and velocity field were obtained in high resolution. Through these experiments the following conclusions were obtained.

1. The time-averaged film cooling effectiveness can be measured with PSP method accurately when precise calibration has been conducted.
2. Instantaneous distributions of velocity vectors and film cooling effectiveness were successfully measured simultaneously by acetone LIF and PIV methods with high resolution. Formation of the fine-scale interface between the coolant jet and the mainstream was clearly visualized in the shear layer.
3. Simultaneous and instantaneous measurement of distribution of velocity vectors and film cooling effectiveness near the exit of circular hole with acetone LIF and PIV is very useful to clarify the complicated mixing flow field of film cooling air and the mainstream clear.
4. The simultaneous quantitative measuring methods with PSP, acetone LIF and PIV are useful to confirm the accuracy of the numerical simulation to solve unsteady flow field of a film cooling, such as LES, etc.

Acknowledgements

The authors wish to express our thanks to Mr. T. Kajiuchi and Mr. Y. Egawa for having conducted precise experimental works at our Thermal Science and Engineering Laboratory, and would like to express grateful acknowledgments to the sustained support of Mitsubishi Heavy Industries Ltd., during the course of this research.

References

[1] Fric, T. F., Roshko, A., Vortical structure in the wake of a transverse jet, *J. of Fluid Mechanics*, vol. 279, pp. 1-47, 1994.
[2] Jovanovic, M. B., Lange, H. C. and Steenhoven, A. A., Influence of hole imperfection on jet cross flow interaction, *Inter. J. of Heat and Fluid Flow*, vol. 27, pp. 42-53, 2006.
[3] Morton, B. R., Ibbetson, A., Jets Deflected in a Crossflow, *Exp. Thermal and Fluid Science*, vol. 12, pp. 112-133, 1996.

[4] Kumagai, K., Takeishi, K., Komiyama, M. and Tokunaga, D., "Numerical and experimental research on a mixing process of film cooling air with mainstream", *Proc. Inter. Heat Transfer Conference*, No. FCV-14, 2006.
[5] Coletti, F., Benson, M. J., Ling, J., Elkins, C. J. and Eaton, J. K., Turbulent transport in an inclined jet in crossflow, *Inter. J. of Heat and Fluid Flow*, vol. 43, pp. 149-160, 2013.
[6] Sakai, E., Takahashi, T. and Watanabe, H., Large-eddy simulation of an inclined round jet issuing into a crossflow, *Inter. J. of Heat and Mass Transfer*, vol. 69, pp. 300-311, 2014.
[7] Moffat, R. J., Describing the Uncertainties in Experimental Results, *Exp. Therm. Fluid Sci.*, vol. 1, pp. 3-17, 1988.
[8] Lazano, A., Yip, B. and Hanson, R. K., Acetone: a tracer for concentration measurements in gaseous flows by planer laser-induced fluorescence, *Exp. in Fluids*, vol. 13, pp. 369-376, 1992.
[9] Eckert, E. R. G., Sakamoto, H., and Simon, T. W., The heat/mass transfer analogy factor Nu/Sh, for boundary layers on turbine blade profiles, *Inter. J. of Heat and Mass Transfer*, vol. 44, pp. 1223-1233, 2001.
[10] Kajiuchi, T., Takeishi, K., Oda, Y., and Kumagai, T., Numerical and Experimental Research on the Film Cooling Flow Fields from Circular and Shaped Holes, *Proc., Inter. Gas Turbine Congress*, Paper No. IGTC7 Tokyo TS-109, 2007.